Proceedings of the
44th IEEE Conference on Decision and Control, and
the European Control Conference 2005
Seville, Spain, December 12-15, 2005

Low-Level Finger Coordination for Compliant Anthropomorphic Robot Grippers

Arne Lehmann and Ralf Mikut and Dirk Osswald

***Abstract*— The execution of a grasp process with an anthropomorphic multi-finger robot gripper has to base on an appropriate movement planning and an accurate low-level control strategy. Stability problems may arise, if there is a deviation, e.g. through position, orientation and/or size perturbation of the object, between planned and real executable movement patterns. One opportunity to react to such perturbations is the use of visual information. But if the there is no visual system available or even the object is concealed, e.g. through the robot gripper, the robot arm or another object, then the use of a visual system is insufficient. For this reason a low-level finger coordination depending on the actual state of the grasp (grasp phase) is presented. With this concept it is possible to coordinate the grasp on the level of the low-level controller and therefore to improve the grasp performance.**

I. INTRODUCTION

To successfully execute a desired task with an anthropomorphic multi-finger robot gripper, beside an appropriate movement planning an accurate control strategy is implicitly needed. The aim of the planning is to generate the desired motions and transform them into a series of desired finger joint trajectories (joint angles $\varphi_{r(i,j)}$ and joint torques $M_{r(i,j)}$ with fingers $i = 1, \ldots, n$ and joints $j = 1, \ldots, m_i$, $n_{DoF} = \sum_{i=1}^{n} m_i$ degrees of freedom). Then these trajectories are used as given reference variables for the controller ($2n_{DoF}$-dimensional vector $\mathbf{w}_r^T = (\varphi_{r(i,j)}, M_{r(i,j)})$).

In the last years many control strategies for different kinds of robot grippers and tasks have been presented. The most common ones are compliance- and hybrid force-position control strategies [2], [3], [4], [5], [6]. With this kind of strategies it is possible to control the interaction of the robot gripper with its environment (objects or humans).

A possibility to achieve the movement patterns for a desired task is to use learned grasp sequences demonstrated by humans [7]. During the last years many studies in this research topic have been published [8], [9], [10], [11], [12]. Most of them divide the process of a grasp into a transport motion (Preshape) and a grasp motion. During the transport motion the arm moves towards the object and the hand opens to get prepared for the following grasp motion. During the grasp motion the desired grasp is executed.

This work is supported by the German Research Foundation DFG in the context of the Collaborative Research Center SFB 588 "Learning and Cooperating Multimodal Robots" [1].

A. Lehmann, Institute of Applied Computer Science, Forschungszentrum Karlsruhe, Germany, arne.lehmann@iai.fzk.de

R. Mikut, Institute of Applied Computer Science, Forschungszentrum Karlsruhe, Germany, ralf.mikut@iai.fzk.de

D. Osswald, Institute for Process Control and Robotics, University Karlsruhe, Germany, osswald@ira.uka.de

Problems occur if there is a deviation between the planned and real executable movement patterns. These deviations arise e.g. through position, orientation and/or size perturbation of the object. One opportunity to react to such perturbations is the use of visual information. But in some cases a visual system is not available, e.g. for reasons of economy or even the object is temporarily concealed, e.g. through the robot gripper, the robot arm or another object. For this reason a low-level finger coordination depending on the actual state of the grasp (grasp phase) is presented. It bases on measured or estimated contact forces or torques. This concept improves the coordination of the grasp on the level of the low-level controller.

Section II presents the detailed realization of the low-level finger coordination. To show the capability of the concept simulated grasp studies of an elastic robot gripper with flexible fluid actuators [13], [14] are presented in Section III.

II. LOW-LEVEL FINGER COORDINATION

Fig. 1 shows the structure of the analyzed system including low-level finger coordination, trajectory modification, contact detection, controller and controlled system (robot gripper + object).

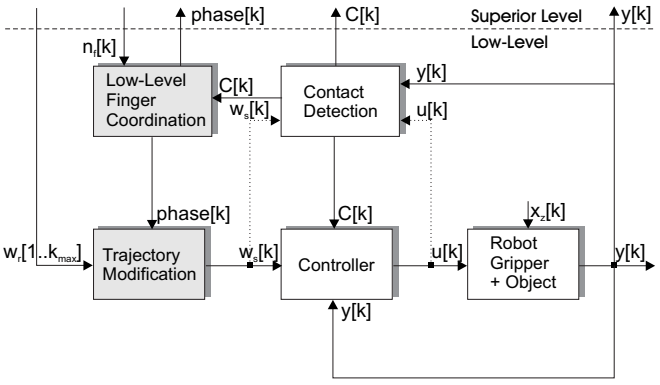

Fig. 1. Time-discrete model structure of the closed-loop system (sampling step k)

For the coordination of a grasp process, it is useful to detect the points in time when the robot gripper gets in contact with the object. Therefore any kind of contact sensors or alternatively a model-based contact detection could be used. If a model-based detection is used, then according to Fig. 1 two additional input variables (dotted), the manipulated variables $\mathbf{u}$ and the reference variables $\mathbf{w}$ are needed to calculate the contact information $\mathbf{C}$.

0-7803-9568-9/05/$20.00 ©2005 IEEE

The superior level defines participating fingers for a grasp. These fingers and the corresponding degrees of freedom will be renumbered ($i = 1, \ldots, n_f, n_{DoF,Part} = \sum_{i=1}^{n_f} m_i$) to simplify the following descriptions. All other fingers remain in their previous phases with their corresponding reference variables and control structures. The main idea of the low-level finger coordination is to introduce phases for the grasp process. The trajectory modification uses these phases to modify the desired finger joint trajectories $\mathbf{w}_r^T = (\varphi_{r(i,j)}, M_{r(i,j)})$ ($2n_{DoF,Part}$-dimensional vector) depending on the grasp phase $\mathbf{phase}^T = (phase_{(i,j)})$ ($n_{DoF,Part}$-dimensional vector). Output values are the modified reference variables $\mathbf{w}_s^T = (\varphi_{s(i,j)}, M_{s(i,j)})$ (Fig. 1).

A Petri Net calculates the actual phase (state) of the grasp (Fig. 2) [15], [16], [17]. Its transitions only depend on the contact information $\mathbf{C}^T = (C_{(i,j)})$.

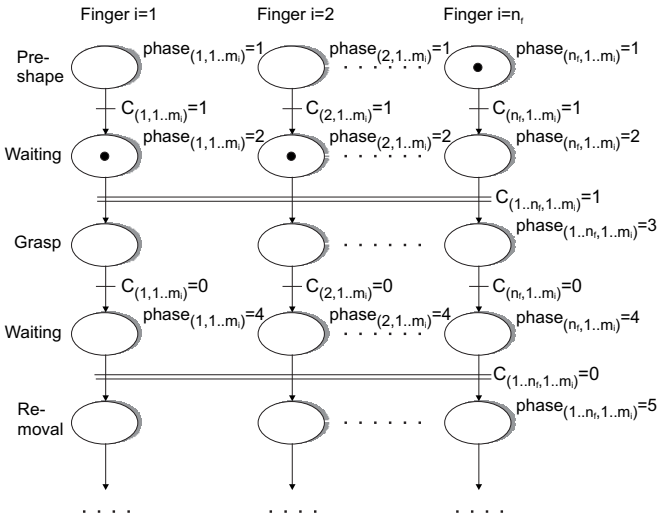

Fig. 2. Petri Net of the low-level finger coordination

During $phase_{(i,j)} = 1$ all participating fingers approach to the object (Preshape). If object contact occurs ahead of time for one or several fingers, e. g. because of position, orientation and/or size perturbation of the object, then these fingers will wait in $phase_{(i,j)} = 2$, since *all* participating fingers arise object contact ($C_{(1..n_f,1..m_i)} = 1$). Subsequently a coordinated grasp process follows ($phase_{(1..n_f,1..m_i)} = 3$). This phase also includes possible transport movements of the object. If it is impossible to reach $phase_{(1..n_f,1..m_i)} = 3$, because of e. g. not predicted object movements or dropping of the object during the grasp, then the low-level finger coordination gives a feedback ($phase_{(1..n_f,1..m_i)} = 3$ not reached) to the superior level, where this exceptional case will be handled. This might lead up to a recurrent planning of the whole grasp sequence [18]. During the removal, all fingers that have lost the contact ahead of time will wait in $phase_{(i,j)} = 4$ for all other participating fingers, followed by a coordinated disengagement ($phase_{(1..n_f,1..m_i)} = 5$).

Starting from these calculated states of the grasp the algorithm shown in Tab. I is used to calculate the modified reference variables $\varphi_{s(i,j)}[k]$ respectively $M_{s(i,j)}[k]$ with k as sampling step and $k = 1, \ldots, k_{max}$ (Fig. 1 Trajectory Modification).

At the beginning of the algorithm the points in time $k_{PC(i,j)}$ when the originally planned contacts should happen and the points in time $k_{PDE(i,j)}$ when the predicted disengagement starts are calculated (Fig. 3):

$$k_{PC(i,j)} = \min k \quad \text{with} \quad M_{r(i,j)}[k] > 0 \tag{1}$$

and

$$k_{PDE(i,j)} = \min k \quad \text{with} \quad \varphi_{r(i,j)}[k] < \varphi_{r(i,j)}[k-1]. \tag{2}$$

For this algorithm the originally planned ramp-shaped trajectories $w_{r(i,j)[1,\ldots,k_{max}]}$ for all sampling steps have to be known in advance. Otherwise a simplified algorithm according to [15] could be used instead.

During $phase_{(i,j)} = 1$ the modified reference variables for the joint angles correspond with the originally planned reference variables:

$$\varphi_{s(i,j)}[k] = \varphi_{r(i,j)}[k]. \tag{3}$$

Because there is no object contact while $phase_{(i,j)} = 1$ the modified reference variables for the joint torques are set to zero:

$$M_{s(i,j)}[k] = const. = 0 \text{ Nm}. \tag{4}$$

If a finger gets in contact with the object, then the points in time $k_{RC(i,j)}$, when the real object contact happens are calculated:

$$k_{RC(i,j)} = \min k \quad \text{with} \quad C_{(i,j)}[k] \neq 0. \tag{5}$$

During $phase_{(i,j)} = 2$ the modified reference variables remain on the values at the points $k_{RC(i,j)}$. This leads to:

$$\varphi_{s(i,j)}[k] = \varphi_{r(i,j)}[k_{RC(i,j)}]. \tag{6}$$

To avoid the loss of contact, the reference variables for the joint torques are set to:

$$M_{s(i,j)}[k] = M_{hold(i,j)} = const. > 0 \text{ Nm}. \tag{7}$$

During $phase_{(i,j)} = 3$ the reference variables for the joint angles remain on the values of $phase_{(i,j)} = 2$ and the originally planned trajectories for the joint torques from the points in time $k_{PC(i,j)}$ are executed (Tab. I, $phase_{(i,j)} = 3$). Therefore an additional point in time k_{SP3} is used, which marks the time when $phase_{(i,j)} = 3$ occurs:

$$k_{SP3} = \min k \quad \text{with} \quad \forall phase_{(i,j)}[k] = 3. \tag{8}$$

During $phase_{(i,j)} = 4$ the trajectories for the joint torques are set to:

$$M_{s(i,j)}[k] = M_{release(i,j)} = const. < 0 \text{ Nm}. \tag{9}$$

This step supports the coordinated disengagement.

During $phase_{(i,j)} = 5$ the points in time $k_{EQ(i,j)}$, when the reference variables for the joint angles are equal to the reference variables of the joint angles at the calculated points $k_{RC(i,j)}$ (5)

$$k_{EQ(i,j)} = k \quad \text{with} \quad \varphi_{r(i,j)}[k] = \varphi_{r(i,j)}[k_{RC(i,j)}] \tag{10}$$

TABLE I

MODIFICATION OF THE REFERENCE VARIABLES $M_{r(i,j)}$, $\varphi_{r(i,j)}$ IN DEPENDENCY OF THE GRASP PHASES (1-5).

Grasp phase	Modification of the reference variables
$phase_{(i,j)}[k] = 1$	$\varphi_{s(i,j)}[k] = \varphi_{r(i,j)}[k]$ $M_{s(i,j)}[k] = const. = 0$
$phase_{(i,j)}[k] = 2$	$\varphi_{s(i,j)}[k] = \varphi_{r(i,j)}[k_{RC(i,j)}]$ $M_{s(i,j)}[k] = M_{hold(i,j)} = const. > 0$
$phase_{(i,j)}[k] = 3$	$\varphi_{s(i,j)}[k] = \varphi_{r(i,j)}[k_{RC(i,j)}]$ $M_{s(i,j)}[k] = \begin{cases} M_{r(i,j)}[k_{PC(i,j)} + k - k_{SP3}] & \text{for } k_{PC(i,j)} \leq k_{RC(i,j)} \vee (k_{PC(i,j)} + k - k_{SP3}) \leq k_{max(i,j)} \\ M_{r(i,j)}[k_{max(i,j)}] & \text{else} \end{cases}$
$phase_{(i,j)}[k] = 4$	$\varphi_{s(i,j)}[k] = \varphi_{r(i,j)}[k_{RC(i,j)}]$ $M_{s(i,j)}[k] = M_{release(i,j)} = const. < 0$
$phase_{(i,j)}[k] = 5$	$\varphi_{s(i,j)}[k] = \begin{cases} \varphi_{r(i,j)}[k_{EQ(i,j)} + k - k_{SP5}] & \text{for } k_{EQ(i,j)} \leq k_{PDE(i,j)} \vee (k_{EQ(i,j)} + k - k_{SP5}) \leq k_{max(i,j)} \\ \varphi_{r(i,j)}[k_{max(i,j)}] & \text{else} \end{cases}$ $M_{s(i,j)}[k] = M_{release(i,j)} = const. < 0$

are calculated and the originally planned reference variables for the joint angles from the calculated points $k_{EQ(i,j)}$ are executed. Therefore an additional point in time k_{SP5} is used, which marks the time when $phase_{(i,j)} = 5$ occurs:

$$k_{SP5} = \min k \quad \text{with} \quad \forall phase_{(i,j)}[k] = 5. \tag{11}$$

The reference variables for the joint torques remain at

$$M_{s(i,j)}[k] = M_{release(i,j)} = const. < 0 \text{ Nm}. \tag{12}$$

To clarify the presented algorithm, Fig. 3 shows the visualization of the calculated points in time $k_{RC(i,j)}$, $k_{PC(i,j)}$, $k_{EQ(i,j)}$, $k_{PDE(i,j)}$, the modified and the originally planned reference variables for the joint angles $\varphi_{s(i,j)}$ (solid), $\varphi_{r(i,j)}$ (dash-dotted) (a.) and for the joint torques $M_{s(i,j)}$ (solid), $M_{r(i,j)}$ (dash-dotted) (b.) as well as the contact situation $C_{(i,j)}$ over the time (c.).

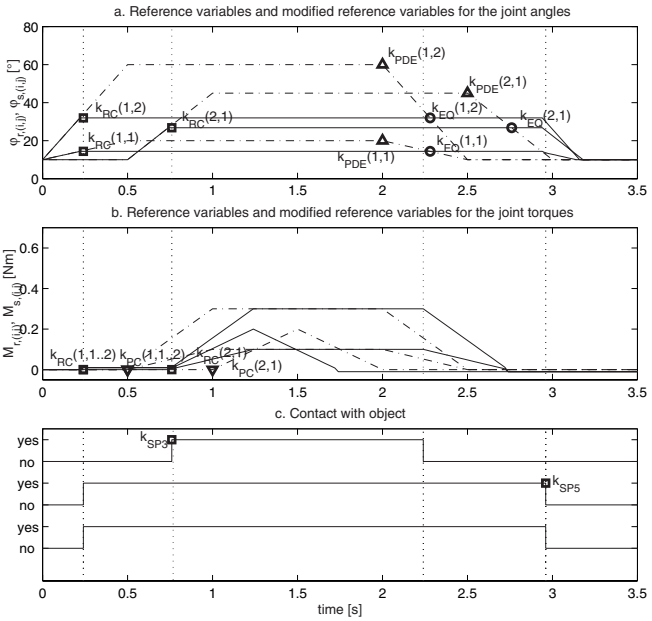

Fig. 3. Example to clarify the effects of the low-level finger coordination

III. APPLICATION

To show the capability of the latter concept (Section II), this section presents simulated grasp studies of an elastic robot gripper with flexible fluid actuators [13], [14]. Therefore the mathematical model of the elastic robot gripper, including the hydraulic system (pump and valves), the mechanical system and the object as well as the developed hybrid force-position control algorithm will be introduced. Fig. 4 shows the structure of the analyzed system including controller, controlled system (robot gripper + object), model-based contact detection as well as the already presented low-level finger coordination and trajectory modification. According to the notations in Fig. 4 this leads to the control variables $\mathbf{y}^T = (\varphi_{(i,j)}, M_{(i,j)})$ with actual joint angles $\varphi_{(i,j)}$ and joint torques $M_{(i,j)}$, the manipulated variables $\mathbf{u}^T = (u_P, u_{V(i,j)})$ (n_{DoF}+1-dimensional vector) with pulse width and direction of the pump u_P and valve positions $u_{V(i,j)}$ (binary on-off or pulse width modulation), the modified reference variables $\mathbf{w}^T = (\varphi_{s(i,j)}, M_{s(i,j)})$ with modified joint angles $\varphi_{s(i,j)}$ and joint torques $M_{s(i,j)}$ and the hydraulic state variables $\mathbf{x}^T = (V_{VB}, V_{A(i,j)})$.

In contrast to conventional robot grippers [19], [20], [21], which are usually powered by electric motors, the elastic 5-finger robot gripper (n_{DoF} degrees of freedom (DOF), m_i joints of the finger number i) of the Research Center Karlsruhe [13], [22] is driven by flexible fluidic actuators. The functional principle bases upon the expansion and contraction of a flexible chamber under pressure, causing

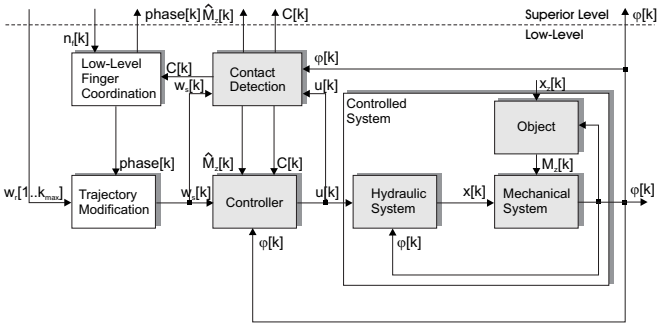

Fig. 4. Model structure of the closed-loop system

the joint torques. A hydraulic system with a pump and n_{DoF} valves controls the pressure in the actuators. The coupled hydraulic and mechanical gripper model [4], [13] is described by a nonlinear differential equation system

$$\ddot{\boldsymbol{\varphi}} = \mathbf{f}(\boldsymbol{\varphi}, \dot{\boldsymbol{\varphi}}, \mathbf{p}_A, \mathbf{x}_z) \tag{13}$$

$$\dot{V}_{VB} = \dot{V}_P(u_P, p_{VB}) - \sum_{i=1}^{n} \sum_{j=1}^{m_i} \dot{V}_{A(i,j)} \tag{14}$$

$$\dot{V}_{A(i,j)} = f_V(p_{A(i,j)} - p_{VB}, u_{V(i,j)}) \tag{15}$$

$$p_{A(i,j)} = f_p(V_{A(i,j)}, \varphi_{(i,j)}), \quad p_{VB} = f_{p,VB}(V_{VB}) \tag{16}$$

with the joint angles $\varphi_{(i,j)}$ and its time derivations $\dot{\varphi}_{(i,j)}$ (n_{DoF}-dimensional vectors: $\boldsymbol{\varphi}, \dot{\boldsymbol{\varphi}}$), the fluid volumes in the actuators $V_{A(i,j)}$ and at the pump V_{VB} as plant states. The pressures in the actuators $p_{A,(i,j)}$ (n_{DoF}-dimensional vector: $\mathbf{p}_A$) and at the pump output p_{VB} are computed from these states. The joint torques $\mathbf{M}_z(\mathbf{x}_z, \boldsymbol{\varphi})$ depend on joint angles, unknown positions and characteristics of (external) contacted objects. They are not directly measurable and will be estimated model-based from the known joint angles and actuator pressures: $\hat{\mathbf{M}}_z(\boldsymbol{\varphi}, \mathbf{p}_A)$.

A cylinder-shaped deformable object is defined through its position in the world coordinate system (WKS, Fig. 5), its radius, its mass and its spring constant k_F (unknown parameters $\mathbf{x}_z$ for the controller) and affects radial forces to the gripper. The simplified friction model includes static and dynamic friction [4].

The controller computes the valve positions $u_{V(i,j)}$ (binary on-off or pulse width modulation) and the pulse width and direction for the pump u_P:

$$\mathbf{u}(t) = \begin{pmatrix} u_P(k \cdot t_a) & u_{V(1,1)}(k \cdot t_a) & \dots & u_{V(n,m_i)}(k \cdot t_a) \end{pmatrix} \tag{17}$$

for $k \cdot t_a \leq t < (k+1) \cdot t_a$.

It is only updated at $t = k \cdot t_a$ with the sampling time t_a. The pulse width and the direction of the pump are found by a nonlinear PI controller with an optional fuzzy adaptation. These manipulated variables are a compromise for an on-line chosen group of joints. Each joint controller switches between position and torque control depending on contact detection [23] and path planning. It controls the corresponding valve and contributes to the pump controller [4]. Advanced cartesian control concepts are not implemented because the pump causes substantial constraints between the joint controllers.

Because no contact sensors are integrated into the modelled 5-finger robot gripper, in this paper the model-based contact detection presented in [23] is used. Input variables of the model-based contact detection are according to [23] the control variables $\mathbf{y}$, the manipulated variables $\mathbf{u}$ and the reference variables $\mathbf{w}$. Output variables are the calculated contact information $\mathbf{C}$ and the estimated joint torques $\mathbf{M}_z(\mathbf{x}_z, \boldsymbol{\varphi})$.

With this system six grasp sequences with different position and/or size perturbations of the object have been executed. For clarity aspects, here only 2-dimensional scenarios with $n_f = 2$ participating fingers are chosen, but the presented concept is able to handle 3-dimensional scenarios with all five fingers as well. During Scenario 1 the object is situated at the originally planned position with no size perturbations (Fig. 5a). During the Scenario 2 no object contact happens, because the object is situated outside of the workspace of the robot gripper (Fig. 5b). The Scenarios 3 and 4 are used to demonstrate the performance of the low-level finger coordination, when the object is bigger or smaller than planed in advance (Fig. 5c, d.). Finally, during the Scenarios 5 and 6 position and size perturbations of the object occur (Fig. 5e, f). Tab. II shows the object parameters (radius of the object and position of the object according to the world coordinate system WKS) for the six analyzed grasp scenarios.

TABLE II

COMPARISON OF THE OBJECT PARAMETERS FOR THE ANALYZED GRASP SCENARIOS (*: AS IN PLANNED SCENARIO)

Object-parameters	Object Radius r [cm]	Object Position ($p_{x,WKS}$/$p_{y,WKS}$) [cm]
Scenario 1	1.5*	(0/4.75)*
Scenario 2	1.5*	(-0.75/9)
Scenario 3	2.25	(0/4.75)*
Scenario 4	1.125	(0/4.75)*
Scenario 5	1.275	(-0.25/4.75)
Scenario 6	2.25	(0.25/4.75)

According to Tab. II, Fig. 5 shows the visualization of the analyzed grasp sequences (1-6) in starting position.

Tab. III and Tab. IV show the comparison of the analyzed grasp scenarios with and without activated low-level finger coordination (LC). The used evaluation criterions are the achieved phases during the grasp process, thereby the minimal aim of the grasp is to reach the grasp phases 1, 3 and 5 otherwise the grasp process is incomplete, the undesired movement of the object during the grasp process $\Delta x/\Delta y$, the control deviation Q_e and the positioning effort of the controller n_{u_P}/n_{u_V}. To calculate the control deviation, first the deviations of the joint angles $\Delta\varphi_{(i,j)}[k]$ and the joint

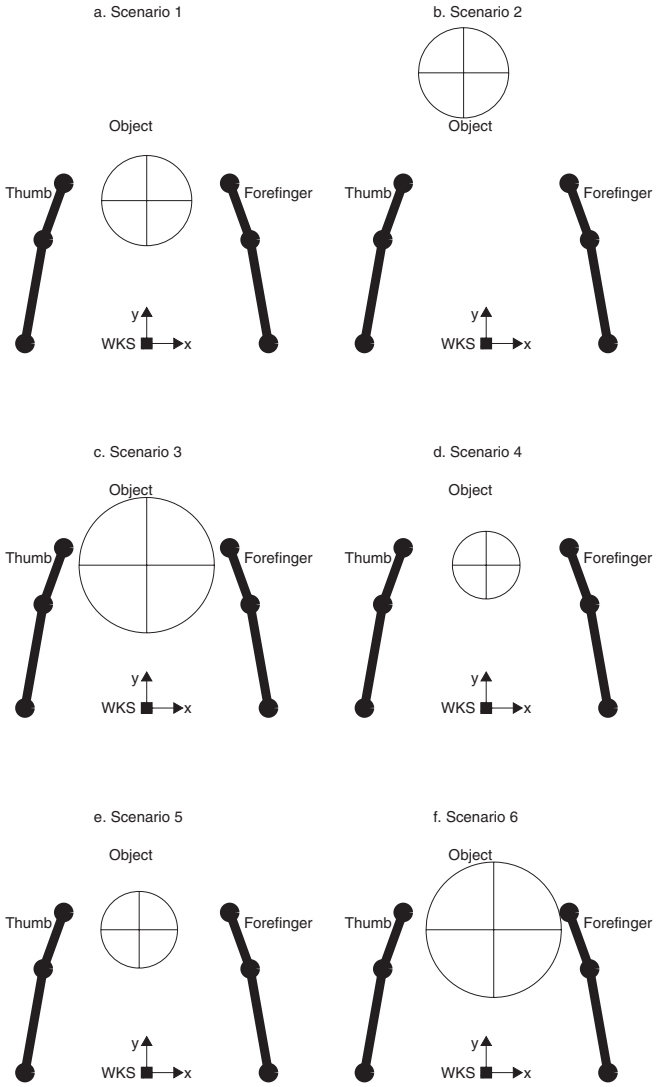

Fig. 5. Visualization of the analyzed grasp scenarios 1-6

torques $\Delta M_{(i,j)}[k]$ are computed:

$$\Delta\varphi_{(i,j)}[k] = \begin{cases} \varphi_{s(i,j)}[k] - \varphi_{(i,j)}[k] & \text{if LC: active} \\ \varphi_{r(i,j)}[k] - \varphi_{(i,j)}[k] & \text{else} \end{cases} \quad (18)$$

and

$$\Delta M_{(i,j)}[k] = \begin{cases} (M_{s(i,j)}[k] - M_{(i,j)}[k]) \cdot K_R & \text{if LC: active} \\ (M_{r(i,j)}[k] - M_{(i,j)}[k]) \cdot K_R & \text{else.} \end{cases} \quad (19)$$

Thereby K_R is a weighting factor to adapt the dimensions of the deviations of the joint torques to the dimensions of the deviations of the joint angles and LC is as short cut for low-level finger coordination. Then the squared deviations are summed over all fingers $i = 1, \ldots, n$, joints $j = 1, \ldots, m_i$ and sampling times $k = 1, \ldots, k_{max}$:

$$Q_e = \sqrt{\sum_{i=1}^{n} \sum_{j=1}^{m_i} \sum_{k=1}^{k_{max}} \Delta\varphi_{(i,j)}^2[k] + \Delta M_{(i,j)}^2[k]}. \quad (20)$$

Finally the positioning effort of the controller is given by:

$$n_{uV} = \sum_{i=1}^{n} \sum_{j=1}^{m_i} \sum_{k=1}^{k_{max}} u_{V(i,j)}[k] \quad (21)$$

$$n_{uP} = \sum_{k=1}^{k_{max}-1} |(\text{sign}(u_{(p)}[k+1]) - \text{sign}(u_{(p)}[k]))| \quad (22)$$

with n_{uV} as sum of all binary valve positions and n_{uP} as sum of all changes of the direction of the pump.

TABLE III

COMPARISON OF ANALYZED GRASP SCENARIOS WITH ACTIVATED LOW-LEVEL FINGER COORDINATION (LC) (GRAY: QUALITATIVE IMPROVEMENTS IN COMPARISON TO TAB. IV)

Scenario	Phases	Pos. Effort		Movement		Dev.
		n_{u_P}	n_{u_V}	Δx	Δy	Q_e
1	[1 3 5]	13	32	0	0.7	7.49
2	[1]	13	40	0	0	1.76
3	[1 3 5]	12	28	0	0.48	10.80
4	[1 3 5]	10	40	0	0.63	9.04
5	[1 2 3 5]	13	40	0.06	0.74	9.10
6	[1 2 3 5]	6	26	0.03	0.6	11.18

TABLE IV

COMPARISON OF ANALYZED GRASP SCENARIOS WITHOUT ACTIVATED THE LOW-LEVEL FINGER COORDINATION

Scenario	Phases	Pos. Effort		Movement		Dev.
		n_{u_P}	n_{u_V}	Δx	Δy	Q_e
1	[1 3 5]	11	40	0	0.71	8.61
2	[1]	13	40	0	0	10.31
3	[1 3 5]	12	40	0	0.80	11.89
4	[1 3 5]	12	48	0	0.58	9.78
5	[1 3]	16	48	0.06	0.67	11.13
6	[1 3]	08	28	0.04	0.87	11.40

The Scenarios 1 and 2 are similar with and without LC. Only the positioning effort and the control deviation for the Scenario 1 with activated low-level coordination are less than for the same scenario without coordination of the fingers.

During the Scenarios 3 and 4, with size perturbations of the object, both fingers achieve the object contact at the same time, but depending on the object being smaller or bigger than planned, for Scenario 3 the contact occurs earlier and for Scenario 4 later than expected. Because the low-level coordination is able to handle these deviations, and modifies the reference variables accordingly, this leads to a smaller control deviation and a smaller positioning effort as well as a less movement of the object.

During the Scenarios 5 and 6, a position and size perturbation of the object is present. This leads to an earlier object contact for the finger which is located nearer to the object. This finger has to wait for the other finger. Without the finger coordination the first finger with object contact (Scenario 5 thumb, Scenario 6 forefinger) executes the planned task and

tries to grasp the object. Because the second finger has not reached the object yet (Scenario 5 forefinger, Scenario 6 thumb), the grasp process is incomplete (Tab. IV, [1 3]). In contrast, with activated finger coordination, a coordinated grasp is possible (Tab. III, [1 2 3 5]). Again this leads to a smaller control deviation and a smaller positioning effort as well as a reduced movement of the object.

As result, the low-level finger coordination successfully performs the grasps in the Scenarios 1, 3-6 (at least grasp phases 1, 3 and 5). Without the activated low-level coordination only the Scenarios 1, 3 and 4 reach the minimal aim of the grasp. In Scenario 2, both strategies must fail because the object is placed outside the workspace of the robot gripper. The low-level finger coordination helps to detect this situation by communicating the phases to the superior level.

Further on the usage of the low-level finger coordination improves the grasp performance, measured through the criterions control deviation and positioning effort of the controller and movement of the object during the grasp, for **all** analyzed scenarios.

IV. CONCLUSIONS AND FUTURE WORKS

A. Conclusions

This paper proposes an easy-implementable concept to coordinate the grasp of a compliant anthropomorphic robot gripper on the level of the low-level controller. To show the capability of the presented concept the algorithm has been applied for a robot gripper with fluidic actuators. Therefore the mathematical descriptions of the hydraulic and mechanic system of the gripper, the object as well as the implemented hybrid torque-position control scheme have been introduced. With this simulation system six grasp sequences with different position and/or size perturbations of the object have been executed and the achieved results have been discussed.

B. Future Works

In further research, the capability of the concept will be analyzed using the real anthropomorphic robot gripper of the SFB 588 "Learning and Cooperating Multimodal Robots" instead of the simulation system.

V. ACKNOWLEDGMENTS

The authors would like to thank Sebastian Beck, Jan Martin, and Tamim Asfour for their help.

REFERENCES

[1] R. Dillmann, "Towards Humanoid Robots in Human-Centered Environments," in *Humanoids 2003 International Conference on Humanoid Robots , Karlsruhe and Munich (Conference Documentation and CD-ROM)*, 2003.

[2] N. Hogan, "Impedance Control: An approach to manipulation," *ASME Journal of Dynamics Systems, Measurement and Control*, vol. 107, pp. 1–24, 1985.

[3] B. Kim, B. Yi, S. Oh, and I. Suh, "Independent Finger and Independent Compliance Control of Multifingered Robot Hands," *IEEE Transactions on Robotics and Automation*, vol. 19,No.2, pp. 185–199, 2003.

[4] A. Lehmann, J. Martin, R. Mikut, and G. Bretthauer, "Konzepte zur Regelung und Stabilitätsüberwachung beim greifen mit flexiblen robotergreifern," in *Proceedings, 13. Workshop Fuzzy Systeme des GMA-Fachausschuss 5.22., Dortmund*, 2003, pp. 79–98.

[5] T. Schlegl, "Diskret-kontinuierliche Regelung mehrfingriger Roboterhände zur robusten Manipulation von Objekten," 2001, Fortschr.-Ber. VDI Reihe 8 Nr. 928. Düsseldorf: VDI Verlag 2002.

[6] L. Sciavicco and B. Siciliano, *Modelling and Control of Robot Manipulators*. Springer Verlag, 2001.

[7] T. Beth, I. Boesnach, M. Haimerl, J. Moldenhauer, K. Bös, and V. Wank, "Analyse, Modellierung und Erkennung menschlicher Bewegungen," in *Proceedings Human Centered Robotic Systems, Karlsruhe*, 2002, pp. 1–8.

[8] M. R. Cutkosky, "On Grasp Choice, Grasp Models, and the Design of Hands for Manufacturing Tasks," *IEEE Transactions on Robotics and Automation*, vol. 5(3), pp. 269–279, 1989.

[9] C. Dohle, "Kinematische Analyse von Greifbewegungen bei Patienten mit Läsionen des parietalen Kortex," Ph.D. Thesis, Heinrich-Heine-Universität Düsseldorf, 2002.

[10] M. Jeannerod, "The neural and behavioural organization of goal-directed movements," *Oxford psychology series*, vol. 15, 1988.

[11] T. Kuhlen, "Entwurf und Validierung eines klinischen Diagnose-Assistenten zur Klassifikation des Greifverhaltens nach realen und virtuellen Objekten," Ph.D. Thesis, RWTH Aachen, 1998.

[12] C. Phillips, "Movements of the hand," *Liverpool University Press*, 1986.

[13] J. Martin, S. Beck, A. Lehmann, R. Mikut, C. Pylatiuk, S. Schulz, and G. Bretthauer, "Sensors, Identification and Low Level Control of a Flexible Anthropomorphic Robot Hand," *International Journal of Humanoid Robotics*, vol. 1(3), pp. 517–532, 2004.

[14] S. Schulz, C. Pylatiuk, and G. Bretthauer, "A new ultralight anthropomorphic hand," in *International Conference on Robotics and Automation, Seoul, Korea*, 2001.

[15] A. Lehmann, R. Mikut, and G. Bretthauer, "Online-Stabilitätsüberwachung strukturvariabler Roboterregelungen," in *VDI-Bericht Nr. 1841*, 2004, pp. 55–63.

[16] R. Mikut, A. Lehmann, and G. Bretthauer, "Fuzzy stability supervision of robot grippers," *Proceeding of the IEEE International Conference on Fuzzy Systems (CD-ROM)*, 2004.

[17] D. Osswald, J. Martin, C. Burghart, R. Mikut, H. Wörn, and G. Bretthauer, "Integrating a Robot Hand into the Control System of a Humanoid Robot," *Robotics and Autonomous Systems*, vol. 48(4), pp. 213–221, 2004.

[18] H.-B. Kuntze, C. Frey, K. Giesen, and G. Milighetti, "On a smart structure variable supervisory control concept for humanoid robots," in *Humanoids 2003 International Conference on Humanoid Robots , Karlsruhe and Munich (Conference Documentation and CD-ROM)*, 2003.

[19] J. Butterfass, M. Grebenstein, H. Liu, and G. Hirzinger, "DLR Hand II: Next generation of a dextrous robot hand." in *International Conference on Robotics and Automation, Seoul, Korea*, 2001.

[20] N. Fukaya, N. Toyama, T. Asfour, and R. Dillmann, "Design of the TUAT / Karlsruhe humanoid hand," in *Proceedings of the IEEE/RSJ ICIRS*, 2000.

[21] C. S. Lovchik and M. A. Diftler, "The robonaut hand: A dexterous robot hand for space." in *Proceedings of the IEEE ICRA*, Detroit, 1999, pp. 907–913.

[22] S. Schulz, C. Pylatiuk, J. Martin, and G. Bretthauer, "Die Anthropomorphe FZK-Hand," in *Robotik 2002 Leistungsstand - Anwendungen - Visionen - Trends (VDI-Berichte 1679)*, 2002, pp. 531–536.

[23] S. Beck, R. Mikut, and G. Bretthauer, "Model-based control and object contact detection for a fluidic actuated robotic hand," *Proceedings IEEE Decision and Control*, 2003.